

Hydroxylation of Specifically Deuterated Limonene Enantiomers by Cytochrome P450 Limonene-6-Hydroxylase Reveals the Mechanism of Multiple Product Formation[†]

Matthias Wüst[‡] and Rodney B. Croteau*

Institute of Biological Chemistry, Washington State University, Pullman, Washington 99164-6340

Received August 23, 2001; Revised Manuscript Received November 26, 2001

ABSTRACT: The regiochemistry and facial stereochemistry of the limonene-6-hydroxylase- (CYP71D18-) mediated hydroxylation of the monoterpene olefin limonene are determined by the absolute configuration of the substrate. (–)-(4*S*)-Limonene is hydroxylated at the C6 allylic position to give (–)-*trans*-carveol as the only product, whereas (+)-(4*R*)-limonene yields multiple hydroxylation products with (+)-*cis*-carveol predominating. Specifically deuterated limonene enantiomers were prepared to investigate the net stereospecificity of hydroxylation at C6 and the mechanism of multiple product formation. The results of isotopically sensitive branching experiments of competitive and noncompetitive design were consistent with a nondissociative kinetic mechanism, indicating that (4*R*)-limonene has sufficient freedom of motion within the active site of CYP71D18 to allow formation of either the *trans*-3- or *cis*-6-hydroxylated product. However, the kinetic isotope effects resulting from deuterium abstraction were significantly smaller than expected for an allylic hydroxylation, and they did not approach the intrinsic isotope effect. (4*S*)-Limonene is oxygenated with almost complete stereospecificity for hydrogen abstraction from the *trans*-6-position, demonstrating rigid orientation during hydrogen abstraction and hydroxyl delivery. The oxygenation of (4*R*)-limonene leading to the formation of (±)-*trans*-carveol is accompanied by considerable allylic rearrangement and stereochemical scrambling, whereas the formation of (+)-*cis*-carveol proceeds without allylic rearrangement and with nearly complete stereospecificity for hydrogen abstraction from the *cis*-6-position. These results demonstrate that a single cytochrome P450 enzyme catalyzes the hydroxylation of small antipodal substrates with distinct stereochemistries and reveal that substrate-dependent positional motion of the intermediate carbon radical (and, therefore, hydroxylation stereospecificity) is determined by active-site binding complementarity. Thus, epimerization and allylic rearrangement are not inherent features of these reactions but occur when loss of active-site complementarity allows increased substrate mobility.

Recent studies with the closely related limonene-3-hydroxylase (CYP71D13) and limonene-6-hydroxylase (CYP71D18) from *Mentha* species (1) have shown that these recombinant cytochrome P450 enzymes (2) control substrate selectivity and hydroxylation regioselectivity by dictating access of the monoterpene olefin substrate, through protein-based steric constraints, to a rather small, and tight-binding, active-site pocket (3, 4). In the case of limonene-3-hydroxylase, both enantiomers of limonene are oxygenated with strict regiochemistry and stereochemistry leading, in mirror image reactions, to *trans*-isopiperitenol. In the case of the C6-hydroxylase, (–)-(4*S*)-limonene is converted to (–)-*trans*-carveol as the only product; with (+)-(4*R*)-limonene as substrate, multiple products are generated, with (+)-*cis*-carveol predominating (Figure 1). This latter observation implies greater intrinsic mobility of the small olefinic

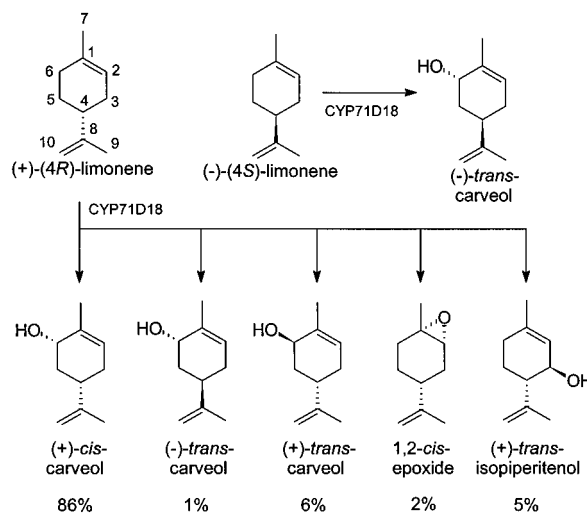


FIGURE 1: Product profiles for CYP71D18-mediated oxidation of (4*R*)- and (4*S*)-limonene.

[†] This work was supported by National Science Foundation Grant MCB-0089472, and by a Humboldt Foundation, Feodor Lynen post-doctoral fellowship to M.W.

* To whom correspondence should be addressed: Phone (509) 335-1790; fax (509) 335-7643; e-mail croteau@mail.wsu.edu.

[‡] Present address: Institut für Lebensmittelchemie, Biozentrum, Universität Frankfurt, 60439 Frankfurt am Main, Germany.

substrate in the active site of limonene-6-hydroxylase (4). It has been proposed that a degree of substrate motion is required for substrate positioning and catalytic function of

cytochrome P450 oxygenases (5); however, a correlation has been observed between substrate mobility and the loss of regioselectivity and hydroxylation efficiency (6), as appears to be the case in comparing the limonene-6-hydroxylase to the highly selective limonene-3-hydroxylase, which also possesses superior kinetics (2, 3).

The evaluation of deuterium KIEs¹ provides a valuable means of assessing substrate mobility and other reaction parameters in cytochrome P450 catalysis (7–9). The magnitude of an observed intramolecular deuterium KIE, which is determined in the oxygenation of two equivalent groups in a substrate that differ only in deuterium substitution, is highly dependent on the rate of positional exchange, which serves as a probe of substrate mobility within the active site (10). Unfortunately, the requirement for structural symmetry in the substrate limits this approach; however, experiments of suitable design nevertheless can provide useful information because the intrinsic KIE can also be unmasked by intramolecular competition between nonidentical sites (9). For these reactions, in which two or more products consequently arise from a single substrate and for which the ratio of products generated is subject to isotopically sensitive branching, the intramolecular KIE (as expressed by alteration of product ratio) can be used to estimate the intrinsic isotope effect (11–13).

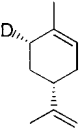
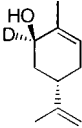
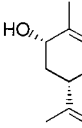
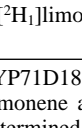
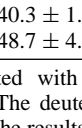
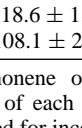
Isotopically sensitive branching experiments can also be utilized to differentiate between possible kinetic mechanisms by which a cytochrome P450 oxygenase catalyzes the formation of multiple products from a single substrate (11, 14, 15). Gillette et al. (16) have devised the means for distinguishing between these kinetic mechanisms by evaluation of the KIEs on the production of deuterium-labeled metabolites that are generated by hydrogen abstraction (see Table 1). Finally, selectively deuterated substrates can be used to investigate stereochemical dynamics of the hydrogen abstraction step of cytochrome P450 catalysis and allow assessment of positional motion of the substrate radical intermediate in the active site (17–19).

In this study, we employ a well-characterized, highly selective, recombinant cytochrome P450 limonene hydroxylase from *Mentha spicata* (1–4) to investigate substrate mobility and reaction stereospecificity by using specifically deuterated limonene isotopomers. This cytochrome P450 system of higher plant origin is particularly well suited for these studies, since it exhibits regioselectivity and stereoselectivity that are substrate-enantiomer-specific. The analysis of deuterium KIEs in this instance has allowed assessment of the kinetic mechanism of multiple product formation from (4*R*)-limonene and provided insight into the stereoselectivity and active-site dynamics for the hydroxylation of small hydrophobic substrates.

EXPERIMENTAL PROCEDURES

Enzyme Preparation and Assay. Procedures for heterologous overexpression in *Saccharomyces cerevisiae* and isolation of the recombinant microsomal limonene-6-hydroxylase (CYP71D18) have been described (2). The protocols for reconstitution with recombinant NADPH:cytochrome P450

Table 1: Stereospecificity of Hydrogen Abstraction in CYP71D18-Mediated Hydroxylation of (4*S*)- and (4*R*)-Limonene

substrate	percentage deuterium content of product ^a (stereoselectivity of protium/deuterium abstraction)	
	trans-6-OH	cis-6-OH
(4 <i>S</i>)-[2H ₁]limonene ^b	81.0 ± 0.4 (97.8 ± 2.1) ^c	not formed
		
(4 <i>R</i>)-[2H ₁]limonene ^b	40.3 ± 1.8 (48.7 ± 4.9)	18.6 ± 1.4 (108.1 ± 2.9) ^d
		

^a CYP71D18 was incubated with (4*S*)-[2H₁]limonene or (4*R*)-[2H₁]limonene at saturation. The deuterium content of each product was determined by GC-MS. The results were corrected for incomplete deuterium incorporation into the labeled substrates and for natural ¹³C isotope abundance and are reported as the mean ± SD of at least three replicates. ^b It should be emphasized that (4*S*)- and (4*R*)-limonene are mixtures of cis- and trans-deuterated isomers: [2H₁]-cis/[2H₁]-trans = 82.8/17.2, as determined by ¹³C NMR spectrometry. By use of the formalism of Ortiz de Montellano and Stearns (28), the calculated and experimental values for the deuterium content of the products can be evaluated with respect to the stereoselectivity of hydrogen removal. ^c It is possible that, due to the primary isotope effect, this stereochemical result underestimates the abstraction of the cis-6-proton that might occur when protium is present at both cis and trans positions. ^d It is possible that, due to the primary isotope effect, this stereochemical result underestimates abstraction of the cis-6-proton.

reductase from *Mentha spicata* (spearmint) (20), and for the hydroxylase assay and extractive product isolation, have also been described (2). All assays were conducted in triplicate, at saturating concentrations of substrate (20 μM), and with appropriate boiled controls. Statistical analyses were performed by applying Student's *t*-test (Microsoft Excel); values of *p* < 0.05 were considered to be statistically significant.

Analytical Procedures. NMR spectra were recorded at room temperature with a Varian Mercury-300BB spectrometer. ¹H NMR was performed at 300.14 MHz (C₂HCl₃/TMS); ¹³C NMR was performed at 75.47 MHz (C₂HCl₃/TMS).

GC-MS analyses of synthetic compounds and enzymatic hydroxylation products were performed with a Hewlett-Packard 6890 GC-MSD (70 eV EI) equipped with 0.25 mm i.d. × 30 m fused silica columns coated with either HP-5MS (0.25 μm df; Hewlett-Packard, Wilmington, DE) or AT-1000 (0.2 μm df; Alltech, Deerfield, IL) with He as carrier at a flow rate of 0.7 mL/min. Cool, on-column injection was used. The oven was programmed from 40 °C (5 min hold) to 230 °C (AT-1000) or to 300 °C (HP-5MS) at 10 °C/min. The stereoselectivity of hydrogen abstraction at C6 in the hydroxylation of (4*R*)- and (4*S*)-[6-²H₁]limonene was determined by monitoring the ratio of [2H₀]- and [2H₁]-(*cis*/*trans*)-carveol at *m/z* 152 and 153, respectively. The products generated in noncompetitive enzyme assays were quantified by use of camphor (40 nmol) as an internal standard (2) (scan range 50–500 amu). The products generated in competitive enzyme assays were determined by selected ion monitoring. With the mixture of (4*R*)-[6-²H₁]limonene and (4*R*)-limonene as substrate, the production of [2H₀]- and [2H₁]-*trans*-isopiperitenol was monitored at *m/z* 152 and 153, respectively. With the mixture of (4*R*)-[3,3,5,5-²H₄]limonene and (4*R*)-limonene as substrate, the production of [2H₀]- and

¹ Abbreviations: df, depth of film; GC, gas chromatography; KIE, kinetic isotope effect; MS, mass spectrometry; NMR, nuclear magnetic resonance (spectrometry).

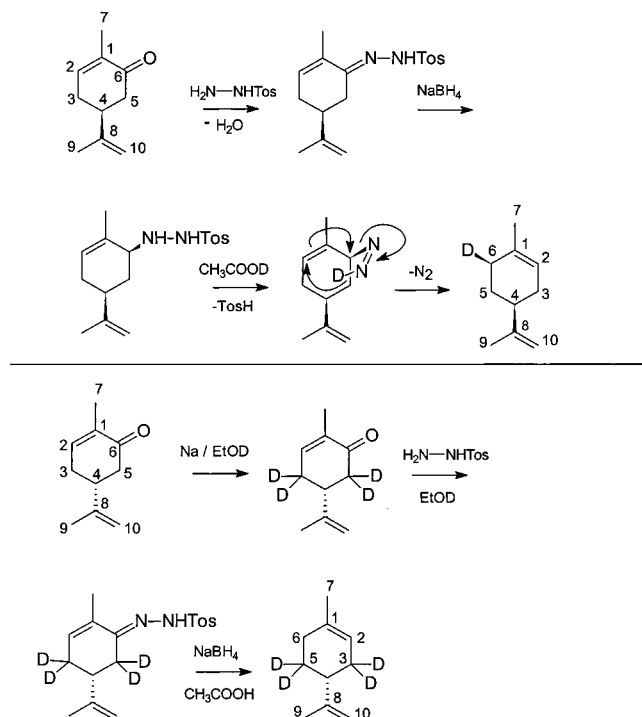


FIGURE 2: Synthesis of (4S)-*cis*-[6- $^2\text{H}_1$]limonene and (4R)-[3,3,5,5- $^2\text{H}_4$]limonene. (4R)-*cis*-[6- $^2\text{H}_1$]limonene was prepared from (R)-carvone as chiral starting material.

[$^2\text{H}_4$]-(*cis/trans*)-carveol was monitored at m/z 152 and 156, respectively, and the production of [$^2\text{H}_0$]- and [$^2\text{H}_3$]-*trans*-isopiperitenol was monitored at m/z 152 and 155, respectively. The exact ratios of (4R)-*cis*-[6- $^2\text{H}_1$]limonene and (4R)-limonene and of (4R)-[3,3,5,5- $^2\text{H}_4$]limonene and (4R)-limonene in the substrate mixtures were determined by assessment of m/z 137 and 136 and of m/z 140 and 136, respectively. The data were corrected for natural ^{13}C abundance, and the exact mole percentage of deuterium incorporation was defined for each substrate and product.

Enantioselective GC analyses of synthetic compounds and enzymatic hydroxylation products were performed with a Hewlett-Packard 5890 chromatograph (flame ionization detector, 300 °C) equipped with a 0.25 mm i.d. \times 30 m fused silica column coated with Rt- β DEX sm (0.25 μm df; Restek Corp., Bellefonte, PA) with H_2 as carrier at a head pressure of 90 kPa. Split injection (220 °C, split ratio 20:1) was employed, and the oven was programmed from 50 °C (5 min hold) to 230 °C at 5 °C/min.

Synthesis of (4R)- and (4S)-*cis*-[$^2\text{H}_1$]Limonene. The labeled limonene enantiomers were prepared by previously described methods (21, 22), by substituting NaBH_4 in $\text{CH}_3\text{COO}^2\text{H}_1$ (98 atom % ^2H) as reactants, to yield *cis*-[6- $^2\text{H}_1$]limonene, for NaB^2H_4 in CH_3COOH , which yield [2- ^2H]limonene. Thus, (S)-carvone (>99%, $[\alpha]_{\text{D}}^{20} + 61.5^\circ \pm 2^\circ$ (neat); Fluka Chemie AG) yielded (4S)-*cis*-[6- $^2\text{H}_1$]limonene, whereas (R)-carvone (~99%, $[\alpha]_{\text{D}}^{20} - 61.5^\circ \pm 2^\circ$ (neat); Fluka Chemie AG) yielded (4R)-*cis*-[6- $^2\text{H}_1$]limonene (see Figure 2). The products were purified by flash chromatography on silica gel with hexane/diethyl ether (100:1 v/v). Enantiomeric purity was 99% (by enantioselective GC); chemical purity was >99% (by GC); *cis/trans*-6- ^2H = 83/17 (by ^{13}C NMR); 91.3% $^2\text{H}_1$, 8.7% $^2\text{H}_0$ (by MS). MS (EI, 70 eV) m/z 137 (M^+ , 11), 136 (1), 122 (19), 108 (17), 94 (64), 93 (63), 80 (64),

53 (66), 68 (100); ^{13}C NMR δ = 150.0 (C8), 133.5 (C1), 120.4 (C2), 108.5 (C9), 41.0 (C4), 30.8 (C3), 30.17 (t, J = 19 Hz, *cis*-C6- ^2H), 30.12 (t, J = 19 Hz, *trans*-C6- ^2H), 27.8 (C5), 23.4 (C7), 20.7 (C10); ^1H NMR δ = 1.66 (q, J = 1 Hz, H7), 1.75 (t, J = 1 Hz, H10), 4.72 (m, H9), 5.40 (m, H2).

Synthesis of (4R)-[3,3,5,5- $^2\text{H}_4$]Limonene. (R)-Carvone (480 mg) was added to 40 mL of EtONa in EtO ^2H (99 atom % ^2H) prepared by dissolving a catalytic amount of Na in anhydrous EtO ^2H under nitrogen. After being stirred for 24 h to substitute exchangeable hydrogens, the reaction was quenched with 2 mL of $^2\text{H}_2\text{O}$, and ethanol was removed under reduced pressure. The product was extracted into pentane (20 mL), and the organic phase was dried over anhydrous Na_2SO_4 . The solvent was removed under reduced pressure, and the exchange-labeled carvone was reductively deoxygenated by an established procedure (21, 22) in which EtO ^2H was substituted for EtOH as solvent in the preparation of the intermediate tosylhydrazone (see Figure 2). The resulting labeled olefin was purified by flash chromatography as above. Enantiomeric purity was >99% (by enantioselective GC); 41.8% $^2\text{H}_4$, 40.9% $^2\text{H}_3$, 15.2% $^2\text{H}_2$, 2.0% $^2\text{H}_1$, <1% $^2\text{H}_0$ (by MS, corresponding to 98% $^2\text{H}_2$ at C3); ^{13}C NMR δ = 150.1 (C8), 133.6 (C1), 120.3 (C2), 108.1 (C9), 41.7 (C4), ~30.3 (quintet, C3; partially overlapping with C6 signal), 30.3 (C6), ~27.2 (m, C5), 23.5 (C7), 20.8 (C10).

RESULTS AND DISCUSSION

Synthesis of Labeled Substrates. (4R)- and (4S)-*cis*-[6- $^2\text{H}_1$]Limonene were prepared in enantiopure form from (R)- and (S)-carvone, respectively, as chiral starting material, via reduction of the corresponding tosylhydrazone in $\text{CH}_3\text{COO}^2\text{H}$ (Figure 2). ^{13}C NMR spectrometry demonstrated that the reduction yielded *cis*-[6- ^2H]limonene stereoselectively (*cis*:*trans* = 83:17). Thus, the proton-decoupled ^{13}C NMR spectrum of the labeled compound showed two triplets at δ = 30.17 and 30.12 ppm with equal coupling constants of J = 19 Hz due to one-bond $^{13}\text{C}-^2\text{H}$ coupling. These two signals can be assigned unequivocally to the respective *cis* and *trans* deuterium atoms at C6 of limonene. The ratio of these signal intensities (83:17) therefore equals the *cis*:*trans* ratio of deuterium atoms at C6 because the nuclear Overhauser enhancement from proton decoupling is the same at a given site and is independent of the number of attached protons (23). The stereochemistry of reduction of the tosylhydrazone can be rationalized by assuming initial α -delivery of hydride to yield the *cis*-hydrazide, since hydride reduction of 5-substituted 2-cyclohexen-1-ones yields chiefly the *cis* isomer (24). The diazene intermediate decomposes with β -facial transfer of deuterium and double-bond migration to yield the *cis*-labeled limonene. The stereoselectivity of tosylhydrazone reductions of cyclohexenone derivatives has been similarly exploited in the synthesis of 9,10-*syn*-diterpenes (25).

(4R)-[3,3,5,5- $^2\text{H}_4$]Limonene was prepared in a similar manner by reductive deoxygenation of (R)-carvone following base-catalyzed exchange of the acidic protons of this ketone in EtONa/EtO ^2H (Figure 2). Time-course studies showed that the protons at C5 (α to the carbonyl) of carvone were completely exchanged (>99%) after 1 h, whereas the exchange of protons at C3 (via the 1,2-double bond) of

carvone occurs at a substantially slower rate. These results are in agreement with previous studies on proton exchange rates in the structurally related monoterpenone piperitone (26, 27). Since reductive deoxygenation of labeled (*R*)-carvone is accompanied by allylic rearrangement, totally labeled C5 of carvone becomes labeled C3 of (4*R*)-[3,3,5,5-²H₄]limonene (98% ²H₂ at C3), and partially labeled C3 becomes partially labeled C5 (42% ²H₂ and 41% ²H₁). The positions of deuterium incorporation were confirmed by ¹³C NMR spectroscopy via the ¹³C–²H couplings as before.

Stereospecificity of Hydroxylation of (4*R*)- and (4*S*)-Limonene. The net stereochemistry of hydroxylation [i.e., of the hydrogen abstracted as well as of the oxygen delivery (18)] mediated by a cytochrome P450 is of mechanistic consequence and can be related to the positional motion of the substrate during the oxygenation reaction. Several cytochrome P450 oxygenations have been investigated with respect to net stereochemistry, and essentially all possible combinations of hydrogen abstraction and oxygen delivery have been observed. For example, the hydroxylation of norbornane by cytochrome P450_{2B4} is accompanied by considerable stereochemical scrambling (17). Thus, both *endo*- and *exo*-alcohols are generated with hydrogen abstraction from the *endo* as well as the *exo* position. The hydroxylation of (+)-camphor by cytochrome P450_{cam} yields, regiospecifically and stereospecifically, only the 5-*exo*-alcohol as product, but hydrogen is removed from either the 5-*endo* or the 5-*exo* position in the process (19). With norcamphor as substrate, 3-*exo*-, 5-*exo*-, and 6-*exo*-alcohols are generated by P450_{cam}, indicating limited regioselectivity; however, nearly complete stereospecificity is observed for *exo*-hydrogen abstraction at C5 and C6 (6). The oxygenation of phenylethane by cytochrome P450_{LM2} affords nearly racemic 1-phenylethanol with either *pro-R* or *pro-S* hydrogen abstraction in both enantiomers (18). Finally, the oxidation of bicyclo[2.1.0]pentane by rat liver microsomes yields *endo*-2-hydroxybicyclo[2.1.0]pentane stereospecifically with *endo* removal of hydrogen and *endo* delivery of the hydroxyl (28). These results demonstrate that net hydroxylation stereospecificity in the hydrogen abstraction and oxygen rebound steps is context-dependent for a particular substrate and P450 protein structure, and therefore provides a useful probe of substrate positional motion relative to the heme iron-bound, active oxygen species of the cytochrome.

The net stereospecificity of limonene-6-hydroxylase (CYP71D18) with (4*S*)-limonene, which is hydroxylated regiospecifically and stereospecifically at the C6 (allylic) position to give (–)-*trans*-carveol as the sole product, and with (4*R*)-limonene, which gives rise to multiple products including (+)-*cis*-carveol, both enantiomers of *trans*-carveol, and (+)-*trans*-isopiperitenol (Figure 1) (4), was evaluated with (4*S*)- and (4*R*)-*cis*-[6-²H₁]limonene as substrates at saturation, and the deuterium content of each enzymatic product was determined by GC-MS (Table 1). The hydroxylation of (4*S*)-*cis*-[6-²H₁]limonene afforded only (–)-*trans*-carveol in which over 97% of the deuterium label was retained at the *cis*-6-position. This nearly exclusive stereoselectivity for *trans*-6-hydrogen removal implies rigid substrate orientation during the hydrogen abstraction step (and during oxygen rebound); however, due to the primary deuterium KIE on abstraction from the *cis*-6-position, this stereochemical result may underestimate the rate of abstrac-

tion of the *cis*-6-proton when protium is present at both positions.

The hydroxylation of (4*R*)-*cis*-[6-²H₁]limonene yielded (+)-*cis*-carveol as the major product, along with both (+)- and (–)-*trans*-carveol, and the deuterium substitution altered the ratio of products due to isotopically sensitive branching (see below). (±)-*trans*-Carveol was generated with loss of almost 50% of the *cis*-6-deuterium label, indicating substantial epimerization involving hydrogen abstraction from both *cis*-6- and *trans*-6-positions. The rate of epimerization indicated by this result (Table 1) could be even higher in the absence of any deuterium KIE on the *cis*-6-hydrogen abstraction. This result implies positional motion of the (4*R*)-limonene substrate during the hydrogen abstraction step, as well as in the oxygen rebound step because oxygen insertion is accompanied by partial allylic rearrangement to produce both enantiomers of *trans*-carveol (4) (see also below). Conversely, the major product (+)-*cis*-carveol was generated with complete deuterium loss from the *cis*-6-position, demonstrating absolute stereospecificity for hydrogen removal from the *cis*-6-position and indicating rigid positioning of the substrate and intermediate during the respective hydrogen abstraction and oxygen rebound steps. These results demonstrate that a single P450 enzyme catalyzes the hydroxylation of antipodal substrates with distinct net stereochemistries, and they reveal substrate-dependent positional motion in the course of the reaction that is controlled by active-site–substrate complementarity (4). Thus, epimerization and allylic rearrangement are not inherent features of these P450-mediated hydroxylations but occur when loss of active-site complementarity allows increased substrate mobility.

Isotopically Sensitive Branching in Limonene Hydroxylation. The product ratios generated by CYP71D18 from (4*R*)-*cis*-[6-²H₁]limonene and (4*R*)-[3,3,5,5-²H₄]limonene are isotopically sensitive, indicating a substantial intramolecular isotope effect (Figure 3). Central to the understanding of this phenomenon, termed metabolic switching or isotopically sensitive branching, is the recognition that a “compensatory shift” in the concentration of enzyme participating in each reaction pathway cancels out rate differences that arise from events after the first irreversible step and that tend to mask the intrinsic isotope effect (29). The theoretical basis for the interpretation of observed kinetic isotope effects in enzymatic reactions, especially those that are isotopically sensitive, has been established (11, 12, 30, 31). Isotopically sensitive branching experiments allow differentiation of the possible kinetic mechanisms by which a single P450 enzyme mediates the formation of several products from the same substrate (16). In the parallel pathway mechanism, the enzyme binds the substrate in several orientations, all of which are essentially static on the enzyme surface and give rise to distinct products (14). In the nondissociative mechanism, different orientations of the substrate in the activated enzyme–substrate complex are interconvertible while the substrate remains in the active site before the hydrogen abstraction step (11). In the dissociative mechanism, the substrate dissociates from the activated complex and reassociates in either the same or different orientations prior to hydroxylation (15). Gillette et al. (16) have derived equations for distinguishing between these kinetic mechanisms by evaluation of deuterium KIEs for substrates that are converted

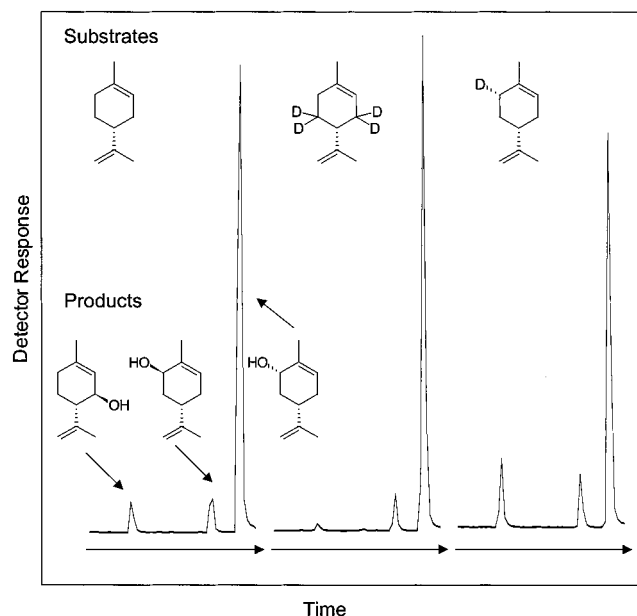


FIGURE 3: GC-MS separation and identification of products generated by CYP71D18-mediated hydroxylation of the three (4*R*)-limonene isotopomers. For clarity, only C3- and C6-hydroxylated products are shown. See Experimental Procedures for analytical details.

to at least two products, one of which is formed by a pathway (P_w) that requires abstraction of deuterium from the labeled substrate, and the other of which is generated by a pathway (P_x) that does not require abstraction of deuterium (Table 2). This approach requires that the isotope effects be determined in both competitive and noncompetitive experiments, and it has been applied thus far to the CYP2C11-mediated oxidation of testosterone (32) and the CYP2D6-mediated oxidation of sparteine (33).

The results obtained with CYP71D18 for the two isotopomers of (4*R*)-limonene from experiments in the competitive and noncompetitive modes are shown in Tables 3 and 4, respectively. Evaluation of the data obtained in competitive experiments (Table 3) clearly indicate that the KIEs on the formation of products that are generated by the nondeuterium abstraction pathway are always less than 1.0, consistent only with a nondissociative kinetic mechanism and indicating that (*R*)-limonene has sufficient freedom of motion within the active site of CYP71D18 to allow the formation of either the *trans*-3-hydroxylated product *trans*-isopiperitenol or the *cis*-6-hydroxylated product *cis*-carveol. However, since hydrogen abstraction at C6 in the formation of *trans*-carveol is not stereospecific (see above), it is not possible to determine the kinetic mechanism that underlies the formation of *cis*- and *trans*-carveol by use of (4*R*)-*cis*-[6- $^2\text{H}_1$]-limonene as substrate. Thus, *cis*-carveol is generated by deuterium abstraction from (4*R*)-*cis*-[6- $^2\text{H}_1$]-limonene as substrate but *trans*-carveol also is generated partially by the deuterium abstraction pathway because the *cis* deuterium, as well as the *trans* proton, are removed [see above; (4*R*)-*trans*-[6- $^2\text{H}_1$]-limonene, which was not synthesized in the present study, would be a suitable substrate for addressing this question]. The KIE on the formation of the *trans*-3-hydroxylated product *trans*-isopiperitenol when (4*R*)-[3,3,5,5- $^2\text{H}_4$]-limonene is used as substrate is normal, as expected. The data from this competitive experiment are consistent because the

Table 2: Expected Deuterium Kinetic Isotope Effects Produced by Different Kinetic Mechanisms

Mechanism ^a	Experiment ^b	
	noncompetitive	competitive
PARALLEL PATHWAY		
$\begin{array}{c} \text{E+S} \rightleftharpoons \text{ES}_w \rightarrow \text{EOS}_w \rightarrow \text{EP}_w \rightarrow \text{E+P}_w \\ \text{E+S} \rightleftharpoons \text{ES}_x \rightarrow \text{EOS}_x \rightarrow \text{EP}_x \rightarrow \text{E+P}_x \end{array}$	1.0	1.0
NONDISSOCIATIVE		
$\begin{array}{c} \text{E+S} \rightleftharpoons \text{ES}_w \rightarrow \text{EOS}_w \rightarrow \text{EP}_w \rightarrow \text{E+P}_w \\ \text{E+S} \rightleftharpoons \text{ES}_x \rightarrow \text{EOS}_x \rightarrow \text{EP}_x \rightarrow \text{E+P}_x \end{array}$	<1.0	<1.0
DISSOCIATIVE		
$\begin{array}{c} \text{E+S} \rightleftharpoons \text{ES}_w \rightarrow \text{EOS}_w \rightarrow \text{EP}_w \rightarrow \text{E+P}_w \\ \text{E+S} \rightleftharpoons \text{ES}_x \rightarrow \text{EOS}_x \rightarrow \text{EP}_x \rightarrow \text{E+P}_x \end{array}$	<1.0 to >1.0	1.0

^a Kinetic mechanisms according to Gillette et al. (16) in noncompetitive experiments for the formation of two different products. For clarity, uncoupling reactions (water and hydrogen peroxide formation) are not included. P_x refers to a product formed by a nondeuterium abstraction pathway, whereas P_w refers to a product formed by a deuterium abstraction pathway. E = enzyme; ES = enzyme-substrate complex; EOS = activated enzyme-substrate complex after cleavage of the oxygen-oxygen bond and release of water; EP = enzyme-product complex. ^b Expected kinetic isotope effects according to Gillette et al. (16) for P_x pathways.

isotope effect on the ratio of the products is larger than is the isotope effect on the formation of *trans*-isopiperitenol (Table 3). The isotope effect on the formation of *cis*-carveol from (4*R*)-*cis*-[6- $^2\text{H}_1$]-limonene could not be determined in the competitive experiment because the deuterium atom is lost during the hydroxylation and the *cis*-carveols thus generated from labeled and unlabeled substrate become indistinguishable.

In the noncompetitive experiments, normal isotope effects were observed for products generated by the deuterium abstraction pathway, and inverse isotope effects were observed for products generated by the nondeuterium abstraction pathway (Table 4), results that again are consistent with a nondissociative kinetic mechanism. The isotope effect on the formation of *trans*-carveol with (4*R*)-*cis*-[6- $^2\text{H}_1$]-limonene as substrate was not significantly different from unity; however, it must be noted that, due to nonspecific hydrogen abstraction (see above), *trans*-carveol is generated in part by the deuterium abstraction pathway, which compensates for an inverse isotope effect. Additionally, abstraction of the *trans*-6-proton might be influenced by a secondary kinetic isotope effect due to change from sp^3 to sp^2 geometry at C6 during catalysis. However, secondary isotope effects in cytochrome P450-mediated benzylic hydroxylations were determined to be quite small (1.09–1.19) compared to the

Table 3: Kinetic Isotope Effects for CYP71D18-Mediated Hydroxylation of (4R)-Limonene in Competitive Experiments

ratio	mean \pm SD ^a
<i>(R)</i> -[² H ₀]Limonene + <i>(R)</i> -[3,3,5,5- ² H ₄]Limonene ^b	
$\frac{(\text{cis-6-OH})_{\text{H}}/(\text{cis-6-OH})_{\text{D}}}{[\text{2H}_0]\text{L}/[\text{2H}_4]\text{L}}$	0.71 \pm 0.17
$\frac{(\text{trans-6-OH})_{\text{H}}/(\text{trans-6-OH})_{\text{D}}}{[\text{2H}_0]\text{L}/[\text{2H}_4]\text{L}}$	0.75 \pm 0.09
$\frac{(\text{trans-3-OH})_{\text{H}}/(\text{trans-3-OH})_{\text{D}}}{[\text{2H}_0]\text{L}/[\text{2H}_4]\text{L}}$	2.53 \pm 0.08
$\frac{(\text{trans-3-OH})_{\text{H}}/(\text{cis-6-OH})_{\text{H}}}{(\text{trans-3-OH})_{\text{D}}/(\text{cis-6-OH})_{\text{D}}}$	3.09 \pm 0.26
$\frac{(\text{trans-3-OH})_{\text{H}}/(\text{trans-6-OH})_{\text{H}}}{(\text{trans-3-OH})_{\text{D}}/(\text{trans-6-OH})_{\text{D}}}$	2.72 \pm 0.50
<i>(R)</i> -[² H ₀]Limonene + <i>(R)</i> - <i>cis</i> -[6- ² H ₁]Limonene ^b	
$\frac{(\text{trans-3-OH})_{\text{H}}/(\text{trans-3-OH})_{\text{D}}}{[\text{2H}_0]\text{L}/[\text{2H}_1]\text{L}}$	0.54 \pm 0.13
$\frac{(\text{cis-6-OH})_{\text{H}}/(\text{cis-6-OH})_{\text{D}}}{[\text{2H}_0]\text{L}/[\text{2H}_1]\text{L}}$	nd ^c
$\frac{(\text{trans-6-OH})_{\text{H}}/(\text{trans-6-OH})_{\text{D}}}{[\text{2H}_0]\text{L}/[\text{2H}_1]\text{L}}$	nd ^d

^a Reported as the mean \pm SD of at least three replicates. ^b CYP71D18 was incubated with equal amounts of *(R)*-[²H₀]limonene and either *(R)*-[²H₄]- or *(R)*-[²H₁]limonene at saturation. The ratio of amounts of each product formed from the unlabeled and labeled substrates was determined by GC-MS and was corrected for incomplete incorporation of deuterium into the labeled substrates during synthesis and for natural ¹³C isotope abundance. The spectrum of the 1,2-epoxide gave no detectable molecular ion, and this minor product was excluded from consideration. ^c The CYP71D18-mediated hydroxylation of *(R)*-*cis*-[²H₁]limonene to *cis*-carveol results in the complete removal of the deuterium label; the corresponding isotope effect in this competitive experiment therefore could not be determined. ^d The CYP71D18-mediated hydroxylation of *(R)*-*cis*-[²H₁]limonene to *trans*-carveol results in partial (nonselective) abstraction of the deuterium label at the *cis*-6-position. The corresponding isotope effect in this competitive experiment therefore could not be determined.

primary component of the deuterium isotope effect (34). Therefore, potential secondary kinetic isotope effects associ-

ated with the hydroxylation of (4R)- and (4S)-[6-²H₁]-limonene were not further considered.

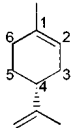
The KIE on the formation of *trans*-carveol with (4R)-[3,3,5,5-²H₄]limonene as substrate was also not significantly different from unity. This observation can be explained by the small branching effect on the formation of this minor product; the analytical methods are not sufficiently accurate to detect the slight shift. It should be noted also that the noncompetitive experiments were carried out at saturating substrate concentrations and therefore represent ^DV_{max} isotope effects. However, Northrop (29) has shown that for reactions in which two or more products arise from one substrate and for which the ratio of products is isotopically sensitive, ^Dv_i resembles ^D(V/K_m) regardless of substrate concentration and is controlled only by commitments to catalysis C_{if} and C_r:

$$^D v_i = \frac{^D k + C_{\text{if}} + C_{\text{r}} ^D K_{\text{eq}}}{1 + C_{\text{if}} + C_{\text{r}}} \quad (1)$$

Thus, in this special case, intramolecular isotope effects are independent of substrate concentration and yield identical values when calculated from v_i, V_{max}, or V_{max}/K_m data; experimental confirmation has been provided in several studies (33, 35, 36). Additionally, intramolecular and intermolecular KIE experiments of competitive and noncompetitive design were recently used to evaluate the energetics and linear free-energy relationships of cytochrome P450-mediated reactions (37).

The highest normal deuterium KIE in the noncompetitive experiments was determined to be 3.21 \pm 0.14 for the formation of the *trans*-3-hydroxylated product from (4R)-[3,3,5,5-²H₄]limonene (Table 4). When this value was corrected for isotopically sensitive branching to the *cis*-6-hydroxylated product by use of the equation ^Dv = [(v_{trans-3-OH})_H/(v_{cis-6-OH})_H]/[(v_{trans-3-OH})_D/(v_{cis-6-OH})_D], a value of 3.68 \pm 0.15 was obtained [by use of the same approach for the *cis*-6-hydroxylated product derived from (4R)-*cis*-[6-²H₁]limonene, a value of ^Dv = 2.83 \pm 0.10 was obtained]. According to Gillette et al. (16), this value should approach the intrinsic deuterium isotope effect if the rates for the interconversion of EOS_{trans-3-OH} and EOS_{cis-6-OH} are much greater than the rates at which these species are reduced to ES_{trans-3-OH} and ES_{cis-6-OH} or converted to EP_{trans-3-OH} and EP_{cis-6-OH} (cf Table 2). By use of the isotopically sensitive

Table 4: Kinetic Isotope Effects for CYP71D18-Mediated Hydroxylation of (4R)-Limonene in Noncompetitive Experiments

substrate ^a	rate ^b (KIE)			
	cis-6-OH	trans-6-OH	trans-3-OH	cis-1,2-epoxide
	25.15 \pm 0.25	1.99 \pm 0.21	1.43 \pm 0.13	0.55 \pm 0.04
<i>(R)</i> - <i>cis</i> -[6- ² H ₁]limonene	17.3 \pm 0.77 (1.45 \pm 0.05) ^c	2.9 \pm 0.16 (0.95 \pm 0.13) ^d	2.70 \pm 0.04 (0.51 \pm 0.09)	1.04 \pm 0.10 (0.53 \pm 0.12)
<i>(R)</i> -[3,3,5,5- ² H ₄]limonene	29.2 \pm 0.37 (0.86 \pm 0.02)	2.15 \pm 0.07 (0.93 \pm 0.11)	0.45 \pm 0.05 (3.21 \pm 0.14)	0.53 \pm 0.10 (1.05 \pm 0.21)

^a CYP71D18 was incubated with the indicated substrate at saturation. ^b Rates of formation of the indicated products (in nanomoles per minute per nanomole of P450) were determined by GC-MS, and, for both rates and KIEs (in parentheses), the means \pm SD are reported. ^c It is likely that, due to the presence of 17% *(R)*-*trans*-[²H₁]limonene in the substrate, this result underestimates the KIE. ^d CYP71D18-mediated hydroxylation of *(R)*-*cis*-[²H₁]limonene to *trans*-carveol involves partial (nonselective) abstraction of the deuterium label at the *cis*-6-position. The corresponding isotope effect in the noncompetitive experiment therefore is overestimated.

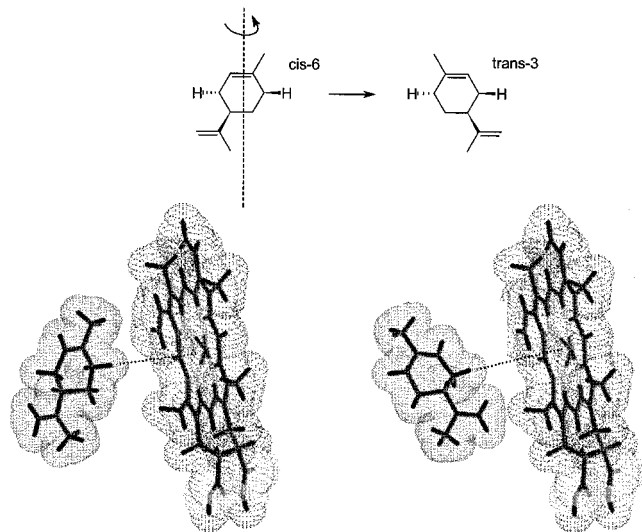


FIGURE 4: Possible substrate orientations in the $ES_{\text{trans-3-OH}}$ and $ES_{\text{cis-6-OH}}$ complex after interconversion of cis-6- and trans-3-protons of (4R)-limonene relative to the heme iron in the active site of CYP71D18.

branching approach, the intrinsic deuterium kinetic isotope effect for an allylic hydroxylation has been estimated to be 7.2 ± 1.0 for radical formation at C6 adjacent to the 4,5-en-3-one system of testosterone (36). Intramolecular deuterium isotope effects for allylic methyl hydroxylation by $P450_{\text{cath}}$ (38) and rat liver microsomes (39) yielded values of 8.0 ± 0.5 and 7.72 ± 0.74 , respectively, and the $P450_{\text{LM2}}$ -mediated allylic hydroxylation of cyclohexene, which is structurally similar to limonene, afforded a deuterium KIE of 5 ± 0.5 when calculated from branching to the cyclohexene epoxide (40).

The value of 3.68 ± 0.15 obtained here is significantly lower than previously reported values for allylic hydroxylations. Thus, the rate constant for the interconversion of $EOS_{\text{trans-3-OH}}$ and $EOS_{\text{cis-6-OH}}$ is probably not sufficiently large to allow full expression of the intrinsic isotope effect, and the KIE value of about 3.7 should be regarded as the lower limit of the true intrinsic deuterium kinetic isotope effect. It is tempting to speculate that the rate of 180° rotation about the symmetry axis of the cyclohexene ring of (4R)-limonene, which is necessary to interconvert the trans-3 and the cis-6 substrate protons at the active site (Figure 4), is significantly reduced by steric constraints imposed by the surrounding amino acid residues. Preliminary, homology-based modeling of the enzyme along with substrate docking experiments² suggest that this rationale is valid and that these steric interactions can be altered by active site-directed mutagenesis (2).

ACKNOWLEDGMENT

We thank Jeffrey Jones for helpful discussions and assistance with the modeling and Joyce Tamura for preparation of the manuscript. The pYedP60 plasmid and WAT11 and WAT21 yeast strains were kindly provided by Denis Pompon (Gif-sur-Yvette, France).

REFERENCES

- Lupien, S., Karp, F., Wildung, M., and Croteau, R. (1999) *Arch. Biochem. Biophys.* 368, 181–192.
- Haudenschild, C., Schalk, M., Karp, F., and Croteau, R. (2000) *Arch. Biochem. Biophys.* 379, 127–136.
- Schalk, M., and Croteau, R. (2000) *Proc. Natl. Acad. Sci. USA* 97, 11948–11953.
- Wüst, M., Little, D. B., Schalk, M., and Croteau, R. (2001) *Arch. Biochem. Biophys.* 387, 125–136.
- De Voss, J. J., Sibbesen, O., Zhang, Z., and Ortiz de la Montellano, P. R. (1997) *J. Am. Chem. Soc.* 119, 5489–5498.
- Atkins, M. A., and Sligar, S. G. (1987) *J. Am. Chem. Soc.* 109, 3754–3760.
- Lu, A. Y. H. (1992) *Front. Biotransform.* 7, 351–363.
- Korzekwa, K. R., Gillette, J. R., and Trager, W. F. (1995) *Drug Metab. Rev.* 27, 45–59.
- Trager, W. F. (1997) *Pharmacochim. Libr.* 26, 275–296.
- Audergon, C., Iyer, K. A., Jones, J. P., Darbyshire, J. F., and Trager, W. F. (1999) *J. Am. Chem. Soc.* 121, 41–47.
- Jones, J. P., Korzekwa, K. R., Rettie, A. E., and Trager, W. F. (1986) *J. Am. Chem. Soc.* 108, 7074–7078.
- Korzekwa, K. R., Trager, W., and Gillette, J. R. (1989) *Biochemistry* 28, 9012–9018.
- Gillette, J. R., and Korzekwa, K. (1991) *Adv. Exp. Med. Biol.* 283, 87–94.
- Grimshaw, C. E., and Cleland, W. W. (1980) *Biochemistry* 19, 3153–3157.
- Harada, N., Miwa, G. T., Walsh, J. S., and Lu, A. Y. H. (1984) *J. Biol. Chem.* 259, 3005–3010.
- Gillette, J. R., Darbyshire, J. F., and Sugiyama, K. (1994) *Biochemistry* 33, 2927–2937.
- White, R. E., Groves, J. T., and McClusky, G. A. (1979) *Acta Biol. Med. Germ.* 38, 475–482.
- White, R. E., Miller, J. P., Favreau, L. V., and Bhattacharyya, A. (1986) *J. Am. Chem. Soc.* 108, 6026–6031.
- Gelb, M. H., Heimbrook, D. C., Mäklönen, P., and Sligar, S. G. (1982) *Biochemistry* 21, 370–377.
- Ponnampuruma, K., and Croteau, R. (1996) *Arch. Biochem. Biophys.* 329, 9–16.
- Hutchins, R. O., and Natale, N. R. (1978) *J. Org. Chem.* 43, 2299–2301.
- Hirata, T., Higata, T., Shimoda, K., Ito, D. I., and Izumi, S. (1997) *J. Label. Comp. Radiopharm.* 39, 285–290.
- Forsyth, D. A. (1984) in *Isotopes in Organic Chemistry* (Buncel, E., and Lee, C. C., Eds.) pp 2–66, Elsevier Science Publishers, Amsterdam, Netherlands.
- Toromanoff, E. (1967) in *Topics in Stereochemistry* (Allinger, N. L., and Eliel, E. L., Eds.) pp 157–198, Interscience Publishers, New York.
- Chu, M., and Coates, R. M. (1992) *J. Org. Chem.* 57, 4590–4597.
- Thomas, A. F., and Willhalm, B. (1967) *J. Chem. Soc. (B)* 1967, 392–400.
- Lamaty, G. (1976) in *Isotopes in Organic Chemistry* (Buncel, E., and Lee, C. C., Eds.) pp 33–88, Elsevier Science Publishers, Amsterdam, Netherlands.
- Ortiz de Montellano, P. R., and Stearns, R. A. (1987) *J. Am. Chem. Soc.* 109, 3415–3420.
- Northrop, D. B. (1991) in *Enzyme Mechanism from Isotope Effects* (Cook, P. F., Ed.) pp 182–198, CRC Press, Boca Raton, FL.
- Northrop, D. B. (1977) in *Isotope Effects on Enzyme-Catalyzed Reactions* (Cleland, W. W., O'Leary, M. H., and Northrop, D. B., Eds.) pp 123–152, University Park Press, Baltimore, MD.
- Northrop, D. B. (1981) *Ann. Rev. Biochem.* 50, 103–131.
- Darbyshire, J. F., Gillette, J. R., Nagata, K., and Sugiyama, K. (1994) *Biochemistry* 33, 2938–2944.
- Ebner, T., Meese, C. O., and Eichelbaum, M. (1995) *Mol. Pharmacol.* 48, 1078–1086.
- Hanzlik, R. P., and Ling, K.-H. J. (1993) *J. Am. Chem. Soc.* 115, 9363–9370.
- Miwa, G. T., Garland, W. A., Hodshon, B. J., and Lu, A. Y. H. (1980) *J. Biol. Chem.* 255, 6049–6054.

² J. P. Jones and R. B. Croteau, unpublished results.

36. Korzekwa, K. R., Trager, W. F., Nagata, K., Parkinson, A., and Gillette, J. R. (1990) *Drug Metab. Disp.* 18, 974–979.
37. Higgins, L. A., Bennett, G., Shimoji, M., and Jones, J. P. (1998) *Biochemistry* 37, 7039–7046.
38. Fretz, H., and Woggon, W.-D. (1986) *Helv. Chim. Acta* 69, 1959–1970.
39. McClanahan, R. H., Huitric, A. C., Pearson, P. G., Desper, J. C., and Nelson, S. D. (1988) *J. Am. Chem. Soc.* 110, 1979–1981.
40. Groves, J. T., Krishnan, S., Avaria, G. E., and Nemo, T. E. (1980) *Adv. Chem.* 191, 277–289.

BI011717H